Using Modeling and Simulation to Assess Challenges and Solutions for 5G Fixed Wireless Access

Gregory J. Skidmore
Remcom, Inc.
State College, PA U.S.

Abstract – A new and innovative modeling and simulation methodology is presented and used to investigate some of the critical challenges that 5G FWA faces for operation at millimeter waves, along with important solutions, such as MIMO beamforming and spatial multiplexing. This approach uses enhanced ray-tracing that captures the full details of polarization and multipath, allowing the assessment of how the environment, the placement of systems, and the use complex MIMO techniques impact a solution's performance. The method also includes estimation of SINR and throughput to provide meaningful metrics for assessment and comparison of alternatives. A case study is carried out for FWA in a suburban neighborhood, using simulations to assess challenges and alternative solutions. The ultimate objectives are to provide insight into key issues faced by FWA as well as to demonstrate a methodology that can be used to assess designs and solutions within realistic, virtual environments.

Index Terms – 5G, MIMO, fixed wireless access (FWA), beamforming, millimeter waves, spatial multiplexing, channel modeling, wireless propagation.

I. INTRODUCTION

Fixed Wireless Access (FWA) is one of the initial planned technologies that may change the digital landscape in the early rollouts of 5G. FWA will provide new and more flexible wireless solutions for broadband for the last mile to homes and businesses. The need for high bandwidth and new spectrum is driving many solutions to consider bands at millimeter wave frequencies; however, this has significant impacts on the ability of signals to propagate to a home or business and penetrate to the interior of buildings to an end user.

A number of alternatives are being considered to address the challenges posed by this application, including placement of the base station and consumer premises equipment (CPE), as well as the use of new and innovative technologies such as *multiple input, multiple output* (MIMO) and beamforming to help overcome high path loss incurred at these higher frequencies. The business case for FWA relies on cost-effective solutions, making careful design and placement of the base stations and CPE's a critical part of making FWA work. Modeling and simulation can provide critical tools to make this analysis possible.

In this paper, a new and innovative modeling and simulation methodology is presented and used to investigate some of the most critical challenges that FWA faces for operation in the physical environment at millimeter waves. This approach uses enhanced ray-tracing that captures the full details of polarization and multipath, allowing the assessment of how the environment, the placement of systems, and the use complex new techniques such as Massive MIMO beamforming impact a solution's performance. The method also incorporates critical effects from the environment, such as the losses from foliage, shadowing from structures, and penetration through building materials, including walls and two-paned glass windows.

Using this methodology, simulations were performed for a fixed wireless access scenario in a suburban neighborhood, and used to evaluate how the locations of base stations and alternative approaches for the placement of CPEs could impact the received signal and the achievable throughput. The objective of the study was to provide insight into some of the key issues faced by FWA, as well as to provide a new proposed methodology for evaluating designs and planning for their placement within realistic environments.

II. SIMULATING CHALLENGES & SOLUTIONS

A. Channel Modeling using Ray-Tracing

For this study, a model based on ray-tracing from Remcom's Wireless InSite® suite was used to predict performance of a MIMO system for a fixed wireless access scenario. This model includes multipath propagation through the outdoor portion of the scene including paths reflecting and diffracting from structures. It also includes transmissions through windows to interior locations. Ray-tracing can generate large numbers of propagation paths between a transmitter and receiver location. The total power from these paths can be expressed as [1]:

$$P_r = \frac{\lambda^2}{8\pi\eta_0}\left|\sum_{i=1}^{N_{paths}}\left[E_{\theta,i}g_\theta(\theta_i,\phi_i) + E_{\phi,i}g_\phi(\theta_i,\phi_i)\right]\right|^2$$

where N_{paths} is the number of propagation paths, E_θ and E_ϕ are theta and phi polarized field components of each path, and g_θ and g_ϕ are the component gains. This method incorporates full three-dimensional multipath effects, including polarization and phase, which is critical for analysis of beamforming and other MIMO techniques.

B. Key Challenges at MM Wave Bands

When compared to wireless communication bands below 6 GHz, millimeter wave bands face several challenges that reduce their performance. Simulation of FWA at these bands must include these effects. Some of these are as follows.

1) High Path Loss and Atmospheric Absorption

Path loss is a basic metric describing propagation loss in free space. When antenna gains are included, this can be expressed as [2]:

$$PL(dB) = 10\log_{10}\left(\frac{P_t}{P_r}\right) = -10\log_{10}\left(\frac{G_tG_r\lambda^2}{(4\pi d)^2}\right)$$

Where G represents transmit and receive gains, λ is the wavelength, and d is the distance a wave has traveled. Because path loss increases inversely with the square of the wavelength, a signal at 28 GHz will suffer approximately 32dB more propagation loss than a signal at 700 MHz, and 18dB more loss than at 3.5 GHz.

Millimeter waves also suffer from atmospheric absorption loss, particularly at specific resonance bands, such as the water vapor resonance near 22 GHz, and the Oxygen resonance near 60 GHz. At the frequencies and ranges in this study, these losses are negligible, but the model includes them nevertheless.

2) Penetration Loss from Vegetation and Structures

Millimeter waves also incur higher penetration loss when propagating through the walls of structures, or through trees and other vegetation. Figure 1 shows sample penetration losses based on material properties from ITU Recommendation p.2040 [3], a 3GPP channel model for LTE [4], and a model for foliage loss by Weissberger [5]. For walls, particularly for newer structures, the loss can be severe, with some materials, like concrete, rising rapidly with frequency. Loss through standard two-pane windows is moderate, which some solutions take advantage of for reception; however, infrared reflective or low-emissivity glass can be much higher, so these can't always be relied on as ports of entry for millimeter waves. Similarly, the Weissberger foliage model suggests that foliage loss through a small number of trees can increase by more than 10 dB over losses at lower frequencies.

In addition to penetration losses, diffractions also fall off rapidly at millimeter wave frequencies, reducing the ability of waves to diffract around structures or trees as they might do at lower frequencies. Because of these losses, millimeter waves perform best in conditions that are in line-of-sight, or close to line of sight with only minor obstructions.

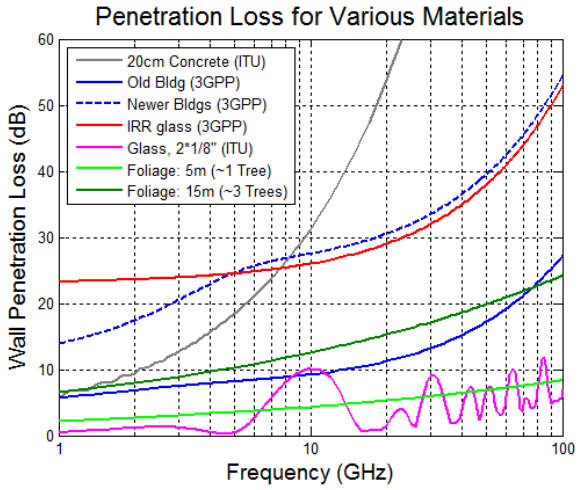

Figure 1 – Penetration Loss for Various Materials

3) Diffuse Scattering

A number of studies in the technical literature indicate that diffuse scattering can also significantly affect the propagation of waves at higher frequency bands ([7], [8]). The models employed in this study include options for diffuse scattering, and some simulations were performed using these models. However, simulations that included diffuse scattering did not significantly alter results of the study and so are not presented in this paper. Future work could include further investigation into the effects of diffuse scattering.

C. Solutions Offered by MIMO Techniques

Some of these disadvantages can be overcome by MIMO techniques, such as beamforming and spatial multiplexing. The small wavelengths allow for arrays with large numbers of antennas, sometimes referred to as *Massive MIMO* arrays, to be designed with a small physical footprint. In the simulation study, the base station was defined with a 128-element array, and two alternative MIMO techniques, beamforming and spatial multiplexing, were assessed to determine their ability to overcome the losses described in the previous section.

To study the potential benefit of beamforming, an adaptive beamforming technique called *maximum ratio transmission* (MRT) was used. This technique uses the channel matrix between the transmitting and receiving antennas to optimize the power at the receiver. The beamforming weighting matrix for a particular receiver, n, is defined as [8]

$$w_n = \frac{h_n}{|h_n|}\sqrt{P_t}$$

where h is the channel vector between the transmitting array and a receiver antenna, and P_t is the total power transmitted by the array. An analogous technique, *maximum ratio combining* (MRC), was applied at the receiver to combine power from the two receive beams, further increasing gain.

In an actual system, it is not possible to achieve perfect knowledge of the channel matrix due to differences in the downlink and uplink chains between the base station and consumer premises equipment. Therefore, the MRT-MRC technique represents an upper bound on how well beamforming could perform under ideal conditions.

To study the benefits of spatial multiplexing, the simulations employed a technique called *singular value decomposition* (SVD), which decomposes the channel into a number of streams equal to the smaller of the number of transmit and receive antennas. This technique uses the channel matrix to determine transmitter precoding and receiver post-coding weights that effectively convert the channel into multiple isolated data streams. The singular value decomposition matrices are defined as [9]

$$H = U\Sigma V^T$$

Where H is the M x N channel matrix (M transmit antennas and N receive antennas). U is an M x M precoding matrix and V is an N x N post-coding matrix, with the superscript "T" denoting the conjugate transpose. $\boldsymbol{\Sigma}$ is the singular value matrix, which is a diagonal matrix whose elements represent the effective channels for the independent data streams. These parallel data streams each contribute to the total throughput.

D. Calculating the Signal-to-Noise Ratio (SNR)

The results of the simulations are presented in terms of the signal-to-interference-plus-noise ratio (SINR), and the estimated data throughput. In the simulations, interference from other base stations was assumed to be negligible, because downlink transmission is using narrow beams, directed toward stationary and spatially separated CPEs, in addition to the fact that millimeter waves suffer high path loss. Therefore, the SINR was effectively the signal-to-noise ratio (SNR).

SNR is simply the ratio of the power to the noise. With MIMO systems, this is calculated from the channel matrix, applying weighting matrices at the transmitter and receiver to perform beamforming or spatial multiplexing as described earlier. Weights applied at the receiver must be applied to the noise as well. The SNR for a MIMO transmitter-receiver pair can be expressed as:

$$SNR = \frac{P_t}{n_t}\frac{|w_r^T\, H\, w_t|^2}{|w_r^T \sigma|^2}$$

where H is the channel matrix, w_t and w_r are the transmitter and receiver weighting matrices, respectively, and σ^2 is the noise power.

E. Estimating Throughput

To estimate the throughput for the scenario, a table mapping throughput to SINR was and used as a user-defined lookup table within the Wireless InSite model. To generate throughput values for the table, the equation specified by 3GPP TS 38.306 V15.2.0 [10] for 5G NR was used to calculate peak throughput based on the modulation order and coding rate for each data stream (or *layer*) calculated by the propagation model. This 3GPP calculation estimates peak throughput for 5G systems, and includes overhead for signaling and control, differentiating the higher frequency bands, such as 28 GHz, and differences between uplink and downlink transmissions. This equation was used to calculate throughput for MCS's from QPSK up to 256 QAM, for a 100 MHz bandwidth with 60 kHz subcarrier spacing, as defined in the 5G NR specification.

Next, combinations of modulation order (QPSK to 256 QAM) and coding rate (0.4 to 1.0 efficiency) were mapped to the SNR required to achieve a sufficiently low block error rate (nominally 1%). This mapping was estimated based on several sources in the literature ([11], [12], [13]) which evaluated relationships between bit error rate and SNR for the modulation coding schemes relevant for 5G NR (QPSK up through 256QAM). The result was a table of throughput as a function of SNR for the 5G 100 MHz component carrier.

As a final step, a factor was applied to account for time-division-duplexing (TDD). Assuming that FWA will be dominated by downlink transmission, it was assumed that approximately 70% of the sub-frames would be used for downlink transmission, and the throughput rates were scaled down accordingly. These steps resulted in a peak downlink throughput of approximately 377 MBps for each layer (stream) of each 100 MHz carrier.

F. Constraints for Fixed Wireless Access Locations

For FWA in a suburban neighborhood, base station antennas are expected to be installed on utility poles or street lights. Utility poles tend to be much higher and will likely perform better in terms of overcoming the propagation challenges described earlier in this paper. Street lights, on the other hand, are more ubiquitous and offer options for a wider variety of neighborhoods. Each alternative height was included in the simulations.

For the CPEs, common locations include roof-top and exterior wall-mounted systems, which would most likely need to be installed by a skilled technician [14]. They also include devices that can be placed by the consumer within a home or business, with the best performance occurring near a window. A third concept that has emerged recently is to include a device that can be mounted on the exterior of a window, where it can capture signals without suffering loss from penetration into the structure, and then transmit to a corresponding device immediately inside the window. This type of system could also be consumer-installed. All three of these concepts were evaluated in this study.

With regard to variability of neighborhoods and cost of deployment, a solution that can successfully operate from a street light height and transmit to a consumer-installed CPE would provide the most flexibility, so the options were evaluated with this goal in mind.

III. RESULTS & DISCUSSION: SIMULATING FWA IN A SUBURBAN NEIGHBORHOOD

A. Suburban Neighborhood FWA Scenario

The simulation methods described in this paper were used to evaluate concepts, challenges, and solutions for a sample FWA scenario in a suburban neighborhood. The scene included one-story and two-story houses, focusing on coverage for homes along a winding neighborhood street, from a single base station placed on the corner at one end of the street. Simulations were performed using Remcom's Wireless InSite® wireless simulation software. Figure 2 provides an image showing homes along the primary street used in the analysis. The simulation included different types of materials for the walls, roofs, and windows of the houses, as well as for streets and grass. A number of areas with trees and vegetation were also defined, shown in the figure as translucent green.

Figure 2 – Suburban FWA Scenario with 3 alternative CPEs: roof-top (left), indoor window sill (middle), and exterior window mount (right)

Analysis was performed for a single base station operating at 28 GHz, with a 100 MHz component carrier bandwidth, consistent with specifications for 5G NR in 3GPP Release 15 [15]. The array consisted of an 8x8 configuration of patch antennas, as shown at the near end of the scene. Each position consisted of cross-polarized elements (± 45 degrees), bringing the total number of antennas to 128.

Consumer premises equipment (CPE) was placed in each of the three alternative configurations described earlier:

- Roof-top mounted (technician installed)
- Indoor, at base of window (consumer placement)
- Exterior, window-mounted (technician or consumer-installed)

Sample locations are shown in the close-ups at the bottom of Figure 2. The roof-top and indoor units were considered as the initial baseline cases. The exterior window-mounted CPE was then evaluated as a potential solution that may be possible for a consumer to install, while providing improved reception over the indoor system.

The same locations were used for each of the houses on the street. For the window units, CPE's were placed in all of the first-story windows of each house, assuming that this is where the equipment would most likely be used.

Table 1 provides some of the basic parameters for the base station and the CPEs. The base station was assessed at two potential heights:

- 12 meters, consistent with the top of a utility pole
- 6 meters, consistent with the top of a street light

The utility pole was used as a baseline, expected to perform better by improving opportunities for line of sight over structures and foliage. The street light, on the other hand, represents a desired option that may be more readily available in many neighborhoods.

CPE antennas were assumed to include adaptive beamforming that would provide some gain. For the indoor CPE, a lower 12 dBi gain was assumed, due to the fact that it will likely require omnidirectional beam steering capabilities. For the exterior window-mounted CPE and the rooftop CPEs, a higher gain of 18dBi was assumed.

Table 1: Parameters for FWA Simulation

Parameter	Definition	Notes
Carrier Frequency	28 GHz	5GNR
Component Carrier Bandwidth	100 MHz	
Base Station Antenna	128-Element MIMO Array	8x8 Patch, with x-pol elements
Transmit Power	37dBm	
B. S. Heights	6 m 12m	Street light Utility pole
CPE Antennas	MIMO (2 beams)	2 x-pol beams
CPE Gains	Low gain: 12 dBi High gain: 18 dBi	Indoor Outdoor
Noise Parameters	Noise: -168dBm/Hz Noise figure: 5dB	
Throughput	TDD peak downlink throughput	Assume 70% DL

B. Performance Metrics: SINR & Throughput

For calculation of SINR, the noise was defined according to measured ambient noise levels in [16] of approximately -168 dBm/Hz for suburban areas. With the 100 MHz bandwidth, this resulted in a -88 dBm noise power, which was further increased by an assumed noise figure of 5dB for each receiver. Interference from other base stations was ignored as discussed earlier in Section II.D.

Downlink peak throughput was estimated from the SINR using curves developed for 5G NR as described earlier in Section II.E, including the assumption of time-division-duplexing (TDD), with the downlink using approximately 70% of the bandwidth. All throughput estimates are for a single 100 MHz component carrier. In an actual system, multiple component carriers would likely be aggregated to achieve the total throughput required for FWA.

C. Baseline Simulations using SISO Configurations

To provide a baseline to assess performance improvements from MIMO and other solutions, initial simulations were performed using single dipole antennas at the base station and CPE locations. This is commonly referred to as single-input-single-output (SISO). This focused on two baseline configurations for the base station and CPE:

- Base station atop utility pole to roof-top CPE
- Base station atop street light to indoor CPE

The first was expected to perform the best, as the higher base stations and CPE positions should make it easier to achieve line-of-sight, but it requires utility poles within the neighborhood and technician installation of the CPEs. The second configuration is expected to face more challenges in propagation of the signal, but is an easier configuration to support, allowing placement of base stations in any neighborhood with street lights, and allowing consumer placement of the CPEs to simplify installation.

SINR for these two baseline configurations is shown in Figure 3, segregated into the left and right sides of the street. Results are presented as a function of range from the base station. The dashed lines represent each individual CPE position at each house along the street. To simplify analysis, the best locations for each house were identified for each CPE type. For the interior window type, for example, the CPE location with the highest SINR was identified for each house (8 on the left, and 9 on the right). These results are displayed as solid lines with markers at the specific optimal locations.

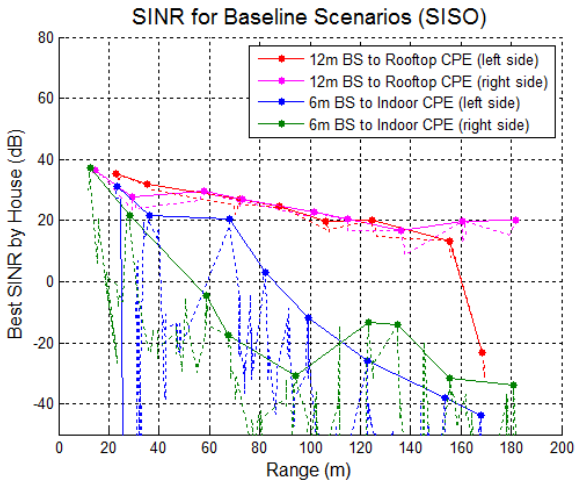

Figure 3 – SINR for Baseline SISO Configurations: (1) Utility pole base station to roof-top CPE, and (2) street light base station to interior window CPE.

The extreme variability for the indoor window locations (green and blue lines) shows how important it is to find a window with a strong signal. Not surprisingly, further analysis showed that the optimal window locations were generally the ones closest to line-of-sight of the base station, as expected.

The results show that the first configuration significantly outperforms the second, with the interior window locations dropping below the noise floor past approximately 40 meters on the right side of the street and past 70 meters on the left, with the right side performing worse due to the presence of more obstructing trees and houses. The taller base station and roof-top CPEs, on the other hand, are able to maintain reasonably-high SINR to all but one of the houses at the very end of the left side of the street, even in this SISO case.

D. Improvement from MIMO Beamforming

Next, massive MIMO beamforming was simulated to evaluate potential improvements to SINR, and the methods described in Section II.D were used to estimate the peak downlink throughput for each case. At the base station, beamforming was simulated using Maximum Ratio Transmission (MRT). At the receiver, the effective gains from receiver beamforming (18 dBi for the roof-top antennas and 12 dBi for the indoor antennas) were applied to form two cross-pol beams, and Maximum Ratio Combining (MRC) was used to further increase the SINR.

Figure 4 shows a comparison of MIMO beamforming simulation results to the SISO baseline for these two cases. The combined beamforming techniques at the transmitter and receiver show significant improvement, achieving 30 to 40 dB increases in the overall SINR for each CPE. This resulted in a corresponding significant improvement to throughput, achieving higher modulation orders (256-QAM) out to 100 meters for the interior window case, and to all but the last house for the utility pole – roof-top CPE case.

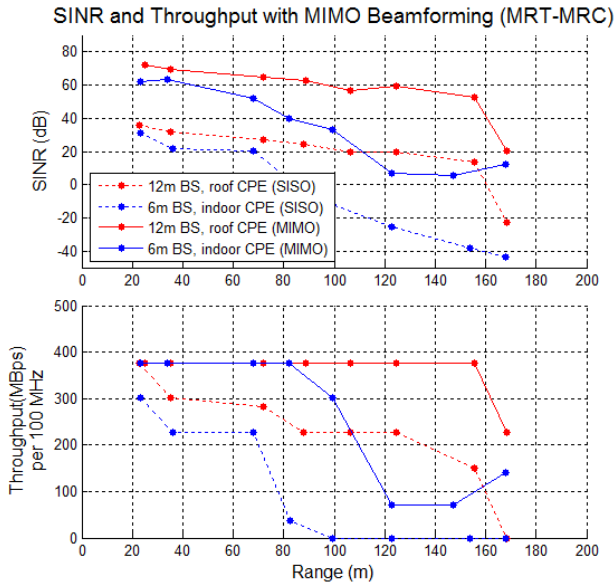

Figure 4 – Improvement to SINR and throughput for baseline cases when beamforming is used. Results are for left side of street.

E. Exterior Window CPE Concept

The exterior window-mounted CPE concept was then evaluated to determine how closely it could match the higher-performing configuration. Because this might be possible for customers to install, it offers most of the same benefits to deployment as the interior window configuration.

The street light base station height was again used, transmitting this time to exterior window-mounted CPEs at each house. The best locations for each house were again determined; these were roughly the same as those for the interior window locations.

Figure 5 shows a comparison of the exterior window-mount locations to the interior windowsill positions for both the left and right sides of the street. This shows improvements of 10 to 20 dB, due partly to the increased gain of the antennas, and partly because there is no longer penetration loss through windows, a loss which varies with angle of incidence (typically higher close to grazing angles).

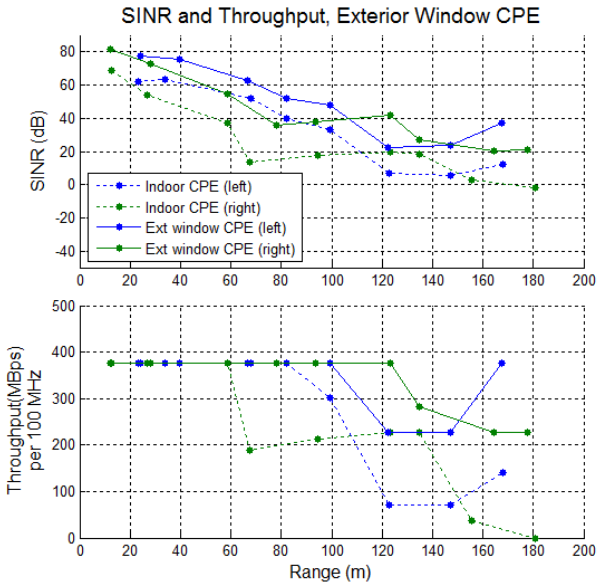

Figure 5 –SINR and throughput for exterior window-mounted CPE, compared to interior window locations

Throughput also improves substantially for the exterior window case. Although the configuration with street light base stations and exterior window-mounted CPEs does not achieve the maximum potential throughput as consistently as for the higher-performance baseline case (utility pole base station and roof-top CPEs), it is able to sustain enough SINR to extend the range of higher throughput levels significantly over the interior windows, and it continues to achieve reasonably high throughput out to the end of the street, for both sides of the street. Table 2 shows results for the full set of base station-CPE combinations, showing the number of houses on the street that are able to achieve progressive levels of throughput.

From these results, it appears that the exterior window-mounted CPE actually performs similarly to the roof-top antennas when comparing for the same base station heights. These results suggest that the exterior window-mounted CPEs provide a reasonable solution for the short-range, suburban neighborhood FWA scenario considered in this study, with the caveat again that the optimal window locations must be found to ensure a window that is close to line-of-sight with the base station.

Table 2: Throughput Achieved by Exterior Window CPE as Compared to other Configurations

Base Station Height	CPE Configuration	Throughput (MBps) # houses (17 on street)		
		> 100	> 200	> 300
12m	Roof-top	17	17	16
	Interior window	16	15	14
	Exterior window	17	17	17
6m	Roof-top	17	17	11
	Interior window	13	11	8
	Exterior window	***17***	***17***	***12***

F. Improvement from Spatial Multiplexing

As a final assessment, MIMO spatial multiplexing was applied to evaluate the potential to increase throughput with parallel data streams. For this study, simulations applied the singular value decomposition (SVD) method described in Section II.C to the channel matrices between the base stations and CPEs for each case. In this scenario, the receiver was assumed to form two cross-polarized beams, allowing support for 2x2 MIMO, potentially doubling the throughput.

Figure 6 shows a comparison of results from spatial multiplexing simulations to those from the earlier beamforming simulations. At closer ranges where the SINR is high, this method is able to double the throughput with two parallel data streams; however, toward the end of the street, the SINR drops substantially, and beamforming is required to maintain a reasonable throughput.

Table 3 compares results for the two MIMO techniques for each type of CPE in terms of the number of houses able to achieve various levels of throughput. Results are for the 6-meter height (street light) base station. Each CPE shows a similar trend, able to achieve much higher throughput with spatial multiplexing for a small number of houses at closer ranges, but performing better with beamforming for houses toward the end of the street, where it is required to sustain SINR for s stronger, single data stream.

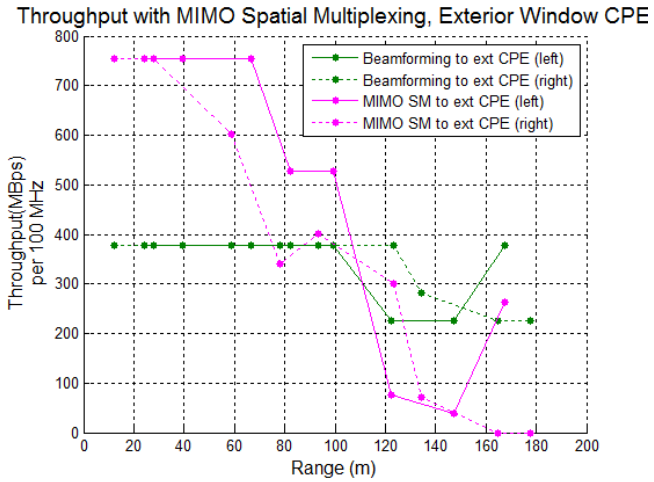

Figure 6 – Comparison of 2x2 MIMO to beamforming for exterior window case. Increases throughput at close ranges, but beamforming performs better toward end of street where required to achieve better SINR.

Table 3: Comparison of Throughput for Spatial Multiplexing vs. Beamforming

Base Sta. Ht.	CPE Config.	Throughput (MBps) # houses (17 on street) > 100	> 200	> 300	>400	>600
6m, BF	Roof-top	17	17	11	-	-
	Int. window	13	11	8	-	-
	Ext. window	17	17	12	-	-
6m, SM	Roof-top	12	11	9	8	5
	Int. window	8	7	6	5	5
	Ext. window	12	12	11	9	6

IV. CONCLUSIONS

This paper has presented a simulation-based methodology for assessing wireless systems for 5G. A case study was carried out using this methodology to assess a fixed wireless access (FWA) scenario in a suburban neighborhood. The goals of the study were to assess challenges for millimeter wave propagation in 5G, and evaluate potential solutions using MIMO beamforming and spatial multiplexing. This included assessing the performance of the system for different potential base station heights and alternative methods for installing the CPEs.

Simulation results show estimates of SINR and peak downlink throughput for several test cases. This study provides some preliminary results for understanding the potential performance of 5G FWA systems within neighborhoods, along with challenges they may face. Future work could evaluate scenarios for other types of neighborhoods, business applications, system designs, or other conditions for the communications network.

V. REFERENCES

[1] *Wireless InSite® 3.3 Reference Manual,* Remcom, Inc., September 2018.

[2] Rappaport, Theodore S., *Wireless Communications: Principles and Practice*. 2nd ed. Upper Saddle River, N.J.: Prentice Hall PTR, 2002.

[3] ITU-R p.2040-1 "Effects of building materials and structures on radiowave propagation above about 100 MHz," July, 2015.

[4] *Study on 3D channel model for LTE*, 3GPP, TR 36.873 (V12.2.0), July 2015.

[5] Weissberger, Mark A., *An Initial Critical Summary of Models for Predicting the Attenuation of Radio Waves by Trees*, Final Report, ESD-TR-81-101, EMC Analysis Center, August 1982.

[6] V. Degli-Esposti, F. Fuschini, E. Vitucci, and G. Falciasecca, "Measurement and modeling of scattering from buildings," IEEE Transactions on Antennas and Propagation, vol. 55, pp. 143–153, January 2007.

[7] V. Degli-Esposti, V.-M. Kolmonen, E. Vitucci, and P. Vainikainen, "Analysis and modeling on co- and cross-polarized urban radio propagation for dual-polarized mimo wireless systems," IEEE Transactions on Antennas and Propagation, vol. 59, pp. 4247–4256, November 2011.

[8] Björnson, E., M. Bengtsson, and B. Ottersten, "Optimal Multiuser Transmit Beamforming: A Difficult Problem with a Simple Solution Structure", *IEEE Signal Processing Magazine*, Vol. 31, No. 4, 2014, pp. 142-148.

[9] Telatar, E. "Capacity of Multi-antenna Gaussian Channels," European Trans. on Telecomm. ETT, 10(6):585–596, November 1999.

[10] *User Equipment (UE) radio access capabilities (Release 15)*, 3GPP TS 38.306 V15.2.0 (2018-06).

[11] D.Vinella, and M. Polignano, "Discontinuous Reception and Transmission (DRx/DTx) Strategies in Long Term Evolution (LTE) for Voice-over-IP (VoIP) Traffic under both Full-Dynamic and Semi-Persistent Packet Scheduling Policies," M.S. Thesis Report, Department of Electronic Systems, Aalborg University, November 20, 2009.

[12] *LTE Transmitter Characteristics*, Telecommunications Industry Association (TIA) technical report WG4-8.18.4_16-05-039-R6, January 2016.

[13] Halawa, T., R. Fathy, and A. Zekry, "Performance Analysis of LTE-A with 256-QAM," 2016 Sixth International Conference on Digital Information Processing and Communications (ICDIPC), 21-23 April 2016.

[14] *Fixed Wireless Access Handbook, Extracted Version*, Ericsson Report EN/LZT 2/28701-FGD 101 449 Uen Rev C, 2018.

[15] *User Equipment (UE) radio transmission and reception; Part 2: Range 2 Standalone (Release 15)*, 3GPP TS 38.101-2 V15.2.0 (2018-06).

[16] Beck, R. *Results of Ambient RF Environment and Noise Floor Measurements Taken in the U.S. in 2004 and 2005*, World Meteorological Organization Report, CBS/SG-RFC 2005/Doc. 5(1), March 2006.